Title

Cranes soar on thermal updrafts behind cold fronts as they migrate across the sea.

Journal

Proceedings of the Royal Society B: Biological Sciences, 291(2015)

Authors

Pekarsky, Sasha

Shohami, David

Horvitz, Nir

et al.

Publication Date

2024-01-31

DOI

10.1098/rspb.2023.1243

Peer reviewed

PROCEEDINGS B

royalsocietypublishing.org/journal/rspb

Research

Cite this article: Pekarsky S, Shohami D, Horvitz N, Bowie RCK, Kamath PL, Markin Y, Getz WM, Nathan R. 2024 Cranes soar on thermal updrafts behind cold fronts as they migrate across the sea. *Proc. R. Soc. B* **291**: 20231243.
https://doi.org/10.1098/rspb.2023.1243

Received: 6 August 2023
Accepted: 11 December 2023

Subject Category:
Ecology

Subject Areas:
behaviour, ecology, environmental science

Keywords:
movement ecology, sea-crossing, mid-latitude cyclones, ecological barrier, soaring-gliding, *Grus grus*

Authors for correspondence:
Sasha Pekarsky
e-mail: sasha.pekarsky@gmail.com
Ran Nathan
e-mail: ran.nathan@mail.huji.ac.il

†These authors contributed equally to this work
‡Current address: Dept. of Environmental Science, Policy & Management, University of California, Berkeley, CA 94720-3114, USA

Electronic supplementary material is available online at https://doi.org/10.6084/m9.figshare.c.6991992.

THE ROYAL SOCIETY PUBLISHING

Cranes soar on thermal updrafts behind cold fronts as they migrate across the sea

Sasha Pekarsky[1,†], David Shohami[1,†], Nir Horvitz[1,‡], Rauri C. K. Bowie[2,3], Pauline L. Kamath[4], Yuri Markin[5], Wayne M. Getz[6,‡] and Ran Nathan[1]

[1]Movement Ecology Laboratory, Department of Ecology, Evolution and Behavior, Alexander Silberman Institute of Life Sciences, The Hebrew University of Jerusalem, Jerusalem 91904, Israel
[2]Museum of Vertebrate Zoology, University of California, Berkeley, CA 94720, USA
[3]Department of Integrative Biology, University of California, Berkeley, CA 94720-3114, USA
[4]School of Food and Agriculture, University of Maine, Orono, ME 04469, USA
[5]Oksky State Reserve, pos. Brykin Bor, Spassky raion, Ryazanskaya oblast 391072, Russia
[6]School Mathematical Sciences, University of KwaZulu-Natal, Durban, South Africa

SP, 0000-0003-4560-2251; DS, 0000-0002-7147-5578; WMG, 0000-0001-8784-9354; RN, 0000-0002-5733-6715

Thermal soaring conditions above the sea have long been assumed absent or too weak for terrestrial migrating birds, forcing obligate soarers to take long detours and avoid sea-crossing, and facultative soarers to cross exclusively by costly flapping flight. Thus, while atmospheric convection does develop at sea and is used by some seabirds, it has been largely ignored in avian migration research. Here, we provide direct evidence for routine thermal soaring over open sea in the common crane, the heaviest facultative soarer known among terrestrial migrating birds. Using high-resolution biologging from 44 cranes tracked across their transcontinental migration over 4 years, we show that soaring performance was no different over sea than over land in mid-latitudes. Sea-soaring occurred predominantly in autumn when large water-air temperature difference followed mid-latitude cyclones. Our findings challenge a fundamental migration research paradigm and suggest that obligate soarers avoid sea-crossing not due to the absence or weakness of thermals but due to their low frequency, for which they cannot compensate with prolonged flapping. Conversely, facultative soarers other than cranes should also be able to use thermals over the sea. Marine cold air outbreaks, imperative to global energy budget and climate, may also be important for bird migration.

1. Introduction

Long-distance avian migrants are hypothesized to select their migratory timing, routes and behaviours in relation to their internal state, the constraints imposed by their motion and navigation capacities, and the environments they pass through [1,2]. Inter- and intraspecific variation in response to environmental conditions is apparently most pronounced when and where migrating birds encounter large ecological barriers such as large seas, oceans or deserts that prevent or restrict migration due to the scarcity of resources and safe habitats and/or the prevalence of environmental conditions that increase the energetic cost associated with crossing [2–5]. Some bird species cross barriers in a straight, continuous flight to minimize the crossing time, some use 'islands' of suitable habitat as stepping-stones for crossing, while others take long detours to either shorten crossing as much as possible or avoid crossing altogether [4,6]. This variation in bird response to ecological barriers depends on several key characteristics such as habitat/food requirements, morphology, physiology and flight mode.

Migrating birds can use two principal flight modes; powered flapping flight during which continuous wingbeats are used to progress and stay aloft, and soaring-gliding during which wings are kept outstretched and the bird alternates

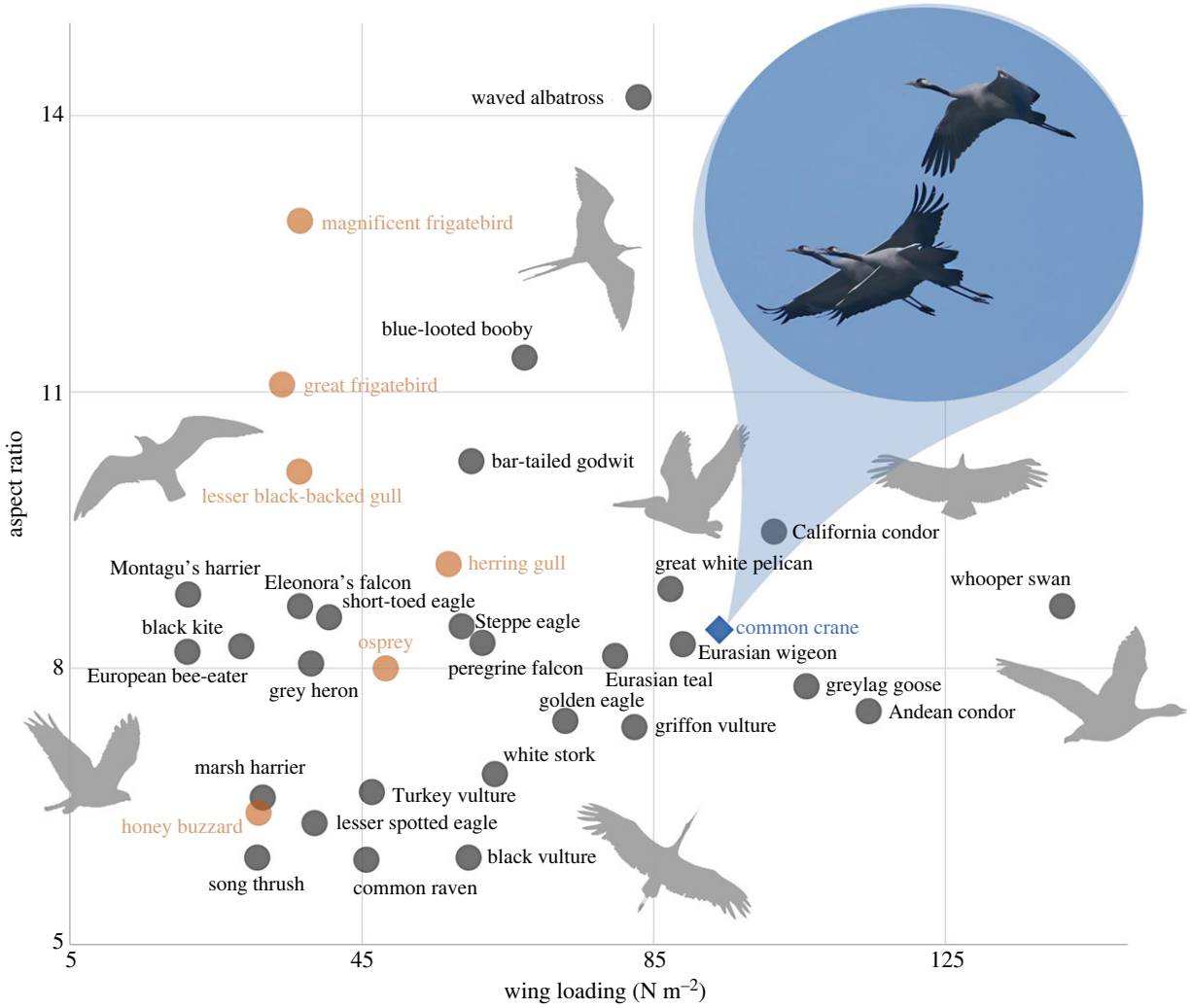

Figure 1. Morphospace defined by the relationship between wing loading and aspect ratio. These two standard morphometrics are known to determine flight performance parameters and soaring-flapping mode [18,19]. The common cranes (blue) are positioned in the morphospace near obligatory soarers such as vultures and obligatory flappers such as geese (morphological data in electronic supplementary material, appendix, table S1). Species known or suspected to perform thermal soaring at sea (orange) generally have lower wing loading compared with cranes. Photo: R. Nathan. Adapted from [18,19].

between a climbing stage and a subsequent descent gliding for forward movement [7–9]. Migration flight strategy represents a continuum of soaring-gliding to flapping, with some species specializing at either end while many others are situated across this continuum. Soaring-gliding flight substantially reduces flight costs by using energy available in the environment [8,9]. However, for land birds, relying on thermal updrafts (columns of rising hot air produced by uneven heating of the ground) for soaring also constrains their migration to regions and times of day where and when thermals are available [4,8,10,11]. Unlike obligate soaring birds that seldom use powered flapping flight, facultative soarers are capable of flapping for a significant part of their flight as well as soaring-gliding, and can thus frequently alternate between flight modes in response to changes in environmental conditions because of their wing morphology and physiology [8,12–14]. Consequently, they can exploit different environments and are less constrained by suitable atmospheric conditions [13–17].

Sea crossing is highly challenging for migrating terrestrial soaring birds that regularly soar and glide over land [4,10], leading to interspecific variation in sea-crossing strategies explained by wing morphology (namely, wing loading) and flight modes (position on the soaring-gliding to flapping continuum) [16,17] (figure 1). Obligate soaring birds take long detours to circumvent the sea [20–22] or cross it only in short sections [23]. White storks (*Ciconia ciconia*), Egyptian vultures (*Neophron percnopterus*) and short-toed eagles (*Circaetus gallicus*), that flap for about 11%, 4% and 2% of their flight, respectively, are exemplary for this behaviour [22,24–27]. The prevailing paradigm in avian migration research assumes that such detours are caused by the absence or weakness of thermal soaring conditions above the sea [4,8,10,11,16,17]. Most terrestrial soaring birds are facultative soarers that are also capable of prolonged flapping and therefore, under the same paradigm, have been assumed to cross the sea exclusively by costly flapping flight [4,10,28].

Nonetheless, ascending air through atmospheric convection does develop over oceans and seas, encompassing atmospheric phenomena such as radiative cooling above cloud tops, trade-wind convection over tropical waters and marine cold air outbreaks outside the tropics [29–31]. In the latter, convection is generated when colder continental air flows over warmer sea-surface water. Under such temperature difference (ΔT; positive if sea surface is warmer than the overlying air), the cold air layer is heated by the water, producing unstable upward-downward air motion in the marine atmospheric boundary layer that may organize into convective cells [29,30]. Recent studies have shown how the unique combination of trade-wind convection over tropical oceans and extreme wing morphology of frigatebirds enables

them to soar as they forage for extended periods [32], and that gulls use soaring flight when foraging at sea relatively close to shore [12]. Yet, despite very early observations of soaring gulls that inspired the meteorological and physical study of cellular convective systems over the oceans [33,34], their utilization for soaring by terrestrial birds over temperate and subtropical waters has been largely ignored in avian migration research [10,11,13] and the paradigm uncontested.

Recent studies have either suggested thermal soaring during sea-crossing based on low-resolution tracking of raptors [35] or examined uplift potential during raptor migration over the sea [36,37], but lacked direct biologging evidence for the circling behaviour typical of thermal soaring. Consequently, sea-crossing solely by flapping flight could not be excluded in these studies. The first, and so far only, direct evidence based on high-resolution GPS tracking comes from ospreys migrating across the Mediterranean Sea [38], which have a relatively low morphospace position (figure 1). Moreover, the underlying meteorological conditions responsible for generating uplift potential that can be (and are) used by migrating birds remain largely under-investigated both in ecological and meteorological studies.

Among migratory birds, cranes are the heaviest facultative soarers that commonly use both low-cost soaring and costly prolonged flapping flight when and where soaring is unfeasible, adjusting their flight mode to the changing atmospheric conditions at their aerial habitat during migration [10,14,17,28]. Cranes have a unique combination of wing morphology traits that neither fit terrestrial nor marine facultative soarers, but lies well within a zone merging the largest obligate soarers (pelicans, vultures and condors) that seldom or never cross the sea, and the largest obligate flapping birds (swans and geese) that use prolonged flapping for sea-crossing (figure 1). Common cranes (*Grus grus*), weighing on average 5.6 kg [39], routinely cross the Baltic, Black, Mediterranean and Red Seas during migration, including long stretches of up to 850 km over open water [28,40]. The common and the white-naped cranes (*Antigone vipio*) are the heaviest facultative soarers known to migrate long distances across the sea and, as in other cases, have been assumed to do so only by flapping flight [10,28,41], but not by thermal soaring.

Here, we used 1524 h of high-resolution (1 Hz) GPS, three-dimensional acceleration and magnetometer measurements from 44 common cranes, tracked along the breadth of their cross-continental migratory route between western Russia and Africa during 2018–2021, to provide the first direct evidence that cranes repeatedly use thermal soaring over the sea far from nearest land. Following this discovery, we set out to investigate their migration flight strategy along their route, comparing different geographical regions over land (northern or southern latitudes) and across the sea (Black or Mediterranean), and between migration seasons (spring or autumn). We then examined how soaring and flapping flight performance and characteristics of the cranes vary over land and sea, and finally investigated the specific meteorological conditions that enable the cranes to soar and glide over extended seascapes.

2. Results

High-resolution biologging of tracked cranes was configured in designated areas over three regions: land north of 32° N, sea (Black and Mediterranean) and land south of 32° N (desert) (figure 2*a*; electronic supplementary material, appendix figure S1). The dataset was divided into 8657 10 min sections, with 3412 sections containing at least one thermal soaring event. Cranes used a combination of flapping and thermal soaring over both land regions and over the sea. In at least 40% of the time, cranes migrated exclusively using flapping flight, even over land at southern latitudes where thermals are assumed to be stronger and frequent (figure 2*b*). The proportion of thermal soaring differed between regions (binomial GLMM, LRTs: region: $\chi^2_4 = 1560$ $p < 0.001$) and seasons (binomial GLMM, LRTs: season: $\chi^2_3 = 149$ $p < 0.001$), with the highest over the desert and lowest over the sea (figure 2*b*(i)), and lower during autumn than spring in the desert but much higher in autumn over the sea (binomial GLMM, LRTs: season×region: $\chi^2_{15} = 148$ $p < 0.001$; figure 2*b*(i)). In diurnal trips with soaring activity, the proportion of time soaring was 2.3 times lower over sea than land (ART-ANOVA: F = 276, $p < 0.001$; figure 2*b*(ii)). The mean (± s.d.) air speed was 10.7 ± 3.9 and 13.1 ± 4.5 m s^{-1} in sections with and without soaring, respectively (ART-ANOVA: F = 201, $p < 0.001$).

Soaring-gliding performance over the sea was not different from that over land at northern latitudes, but both were significantly different from that over land at southern latitudes. More specifically, over the desert, cranes had higher climbing rates and lower flapping ratios in both the climbing and gliding phases (ART-ANOVA: $p < 0.001$; figure 3). Thermal exit height above ground level was significantly higher over the desert than over land at northern latitudes (median height: 725 and 516 m, respectively; ART-ANOVA: $p < 0.001$), but not significantly different over the sea (median height: 594 m) compared with both land regions. The estimated minimum sink rate of common cranes, calculated in the program FLIGHT (version 1.25) [42], is 0.66 m s^{-1}. Thermal uplift strength, which can be regarded as the minimum sink rate added to the soaring climb rate, ranged from approximately 1 to 3.5 m s^{-1}.

The probability of thermal soaring when cranes crossed the sea, a proxy for the probability of thermal formation over the sea, was significantly and positively related to ΔT and wind speed at median flight height (395 m), but the wind speed effect was weak (appendix, electronic supplementary material, table S2). Generally, thermal soaring occurred mostly in ΔT > 1. To understand the broader meteorological context, we examined meteorological conditions 3 days before and 1 day after Mediterranean Sea crossing events during autumn (figure 4*c*). Out of 40 crossing events recorded in high resolution (figure 4*a*), 25 (62%) included at least one thermal soaring event. Cranes that crossed the sea with thermal soaring stayed significantly longer at the last stopover before crossing, compared with birds that crossed without any thermal soaring (ART-ANOVA: $F = 5.9$, $p = 0.02$; figure 4*b*). For events including thermal soaring, environmental conditions 2 and 3 days prior to departure were mostly all significantly different than the departure day and showed clear and significant trends (one-way ANOVA: $p \leq 0.01$ for all variables; figure 4*c* blue lines). By contrast, sea-crossing events that did not include soaring did not show significant trends or differences between days in any of the meteorological variables (one-way ANOVA: N.S; figure 4*c* red lines). ΔT levels were, on average, lowest 3 days before departure of soaring cranes (indicating relatively high air temperature very close to the sea

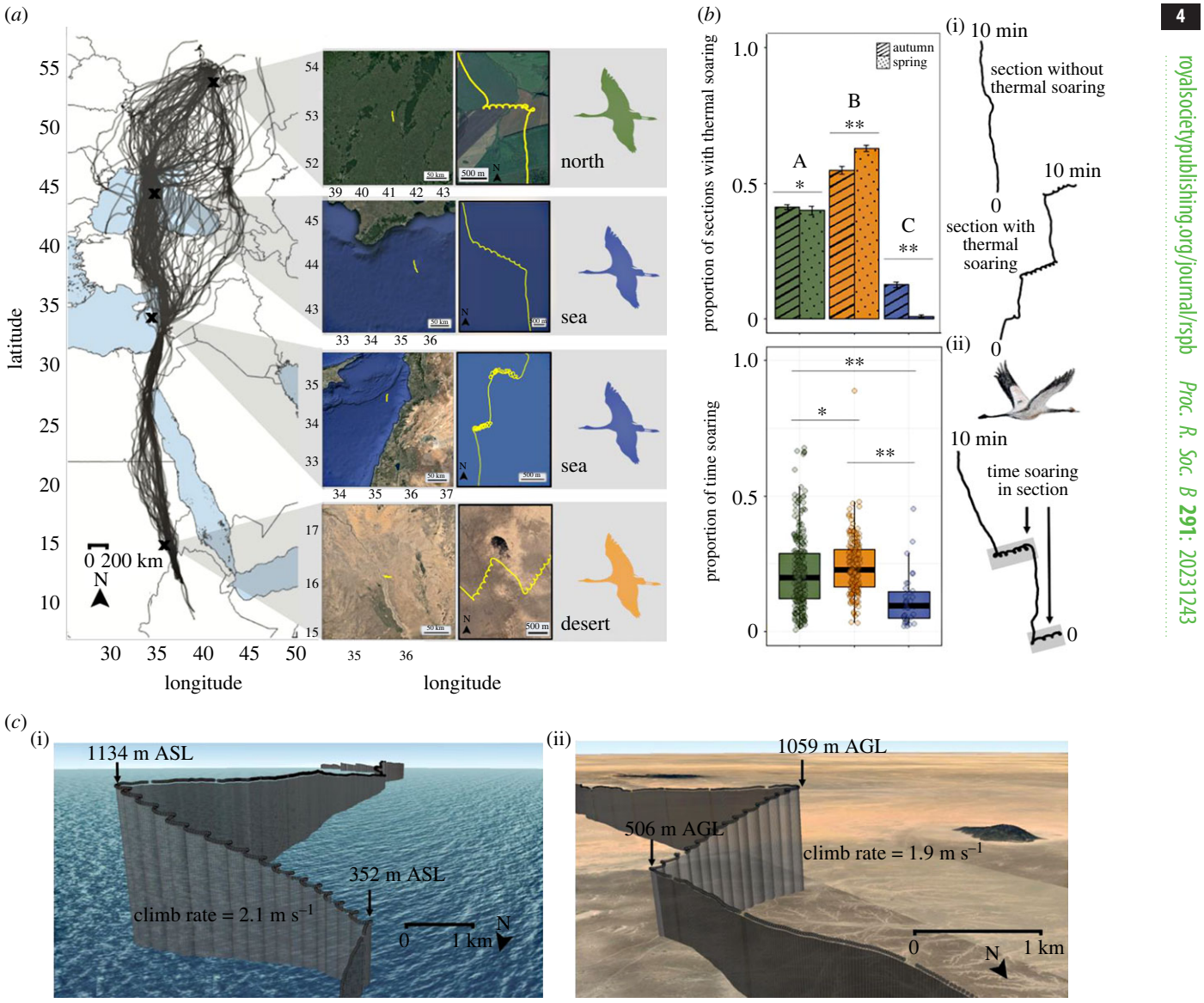

Figure 2. Soaring during migration trips over sea and land. (*a*) GPS tracks of 44 cranes for 135 autumn and spring migrations. To the right, examples of high temporal resolution (1 Hz) 10 min sections with soaring over land north of 32° N (green, 'north'), the Black and Mediterranean Seas (blue) and land south of 32° N (orange, 'desert'). (*b*) (i) proportion of 10 min sections with thermal soaring (climbing) at different geographical regions and seasons. Asterisks and grouping letters represent *post hoc* Holm-adjusted comparisons from binomial GLMM indicating significant difference between seasons and geographical regions, respectively; (ii) proportion of time soaring within 10 min sections during migration days with at least one soaring event. Asterisks indicate significant difference between regions from ART-ANOVA with pairwise Tukey *post hoc* (* $p < 0.05$, ** $p < 0.001$). (*c*) Three-dimensional view of a migratory track segment in 1 Hz above the Black Sea (i) and above the Sahara Desert in Sudan (ii). AGL, above ground level; ASL, above sea level.

temperature, Dunnett's test: $p = 0.07$) and reached a maximum 1 day before departure, indicating a decrease in air temperature. By contrast, crossings without soaring occurred during low ΔT levels without a sharp increasing trend in the preceding days (figure 4*d*). Additionally, crossings that included thermal soaring were preceded by a decrease, followed by a sharp increase, in sea level pressure, on average reaching a minimum 2 days before departure (Dunnett's test: $p < 0.05$). They also occurred during a minimum in total cloud cover and daily precipitation, both reaching a maximum 2–3 days before departure (Dunnett's test: $p = 0.008$ and $p < 0.001$, respectively). Tailwind was present during departure days of soaring cranes, but there was headwind 2 and 3 days prior (Dunnett's test: $p < 0.05$). Since autumn departures for Mediterranean Sea-crossings are in a southerly direction (mean ± s.d. 285° ± 16), tail- and headwinds generally correspond to northerly and southerly winds, respectively. The synoptic interpretation of these results indicates the passing of a mid-latitude cyclone (low-pressure area) and associated cold front 2 days, on average, prior to departures for Mediterranean Sea-crossings that included thermal soaring (figure 4*e*).

3. Discussion

Our data directly demonstrate thermal soaring over the sea by a large, heavy terrestrial migrant, with wing loading up to twice that of all raptors and gulls for which this behaviour was previously documented [33,34,38] or suggested [35–37]. Importantly, we found that soaring crane climb rates and thermal exit heights over the sea were comparable to over land in northern latitudes (figure 3*a*), but the time spent soaring was considerably lower (figure 2*b*), suggesting lower

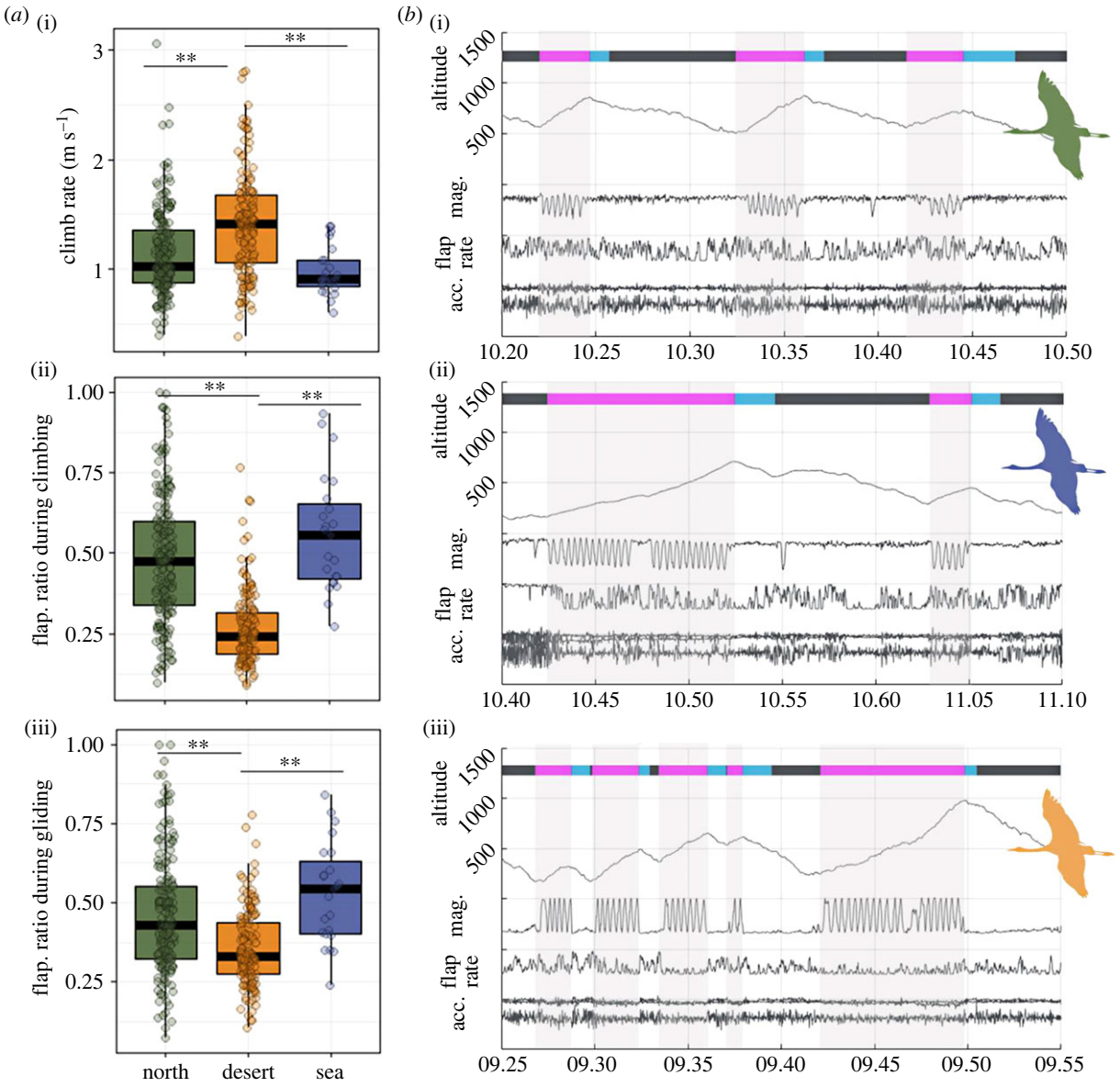

Figure 3. Soaring flight characteristics across three geographical regions. Figure 2 for region classifications and colour codes. (*a*) (i) Climb rate during soaring phase, and (ii and iii) flapping ratio (number of wingbeats out of the maximal number of wingbeats expected during flapping flight; see Methods) during soaring and gliding phases, respectively, based on 1 Hz tri-axial acceleration. Boxplots represent averaged individual data of daily means (for days with more than one soaring-gliding event) with population median of all samples (north, $N = 182$; desert, $N = 154$; sea, $N = 23$). Asterisks indicate significant difference between groups (* $p < 0.05$, ** $p < 0.001$; ART-ANOVA with pairwise Bonferroni *post hoc*). (*b*) Typical ethograms of flight types within a single flight segment classified to circular thermal climbing (pink bar with grey shading) and gliding (blue bar) according to flight height (GPS) and heading change (GPS and magnetometer). Height above ground (m), magnetometer (gauss), mean flap rate (flaps s^{-1}) and tri-axial acceleration (m s^{-2}) shown over the north (i), sea (ii) and desert (iii) regions. Time shown on the *x*-axis is Coordinated Universal Time (UTC).

frequency but not lower strength of thermals over the sea. These findings challenge fundamental assumptions in avian migration research that have assigned a small, if any, role for thermals over the sea for migrating birds and explained sea avoidance of obligate soarers by thermal absence or weakness [4,8,10,11,38,43]. Rather, our findings suggest that lower thermal frequency—hence higher thermal uncertainty—greatly limits obligate soarers and thus better explains their avoidance of sea-crossing, rather than thermal strength. Our findings further imply that not only cranes and ospreys [38], but probably also honey buzzards [36,37] and other facultative soaring species capable of flapping for a significant part of their flight, also use thermal soaring as they cross open seas, allowing a reduction in the energy needed to cross this barrier as well as a reduction in time by avoiding large detours.

Our study shows the ability of facultative soaring migrants to switch flight modes in response to changes in the environmental conditions they encounter *en route*. Common cranes heavily rely on powered flapping flight, use it exclusively for around half of their migratory flights and frequently flap also during thermal soaring-gliding (figures 2*b* and 3). This corresponds to a previous assertion by Pennycuick *et al.* [28] that flapping is the common crane's primary mode of flight. Climb rates reported in [28] are also similar to ours, in the range of 0.5–2.5 m s^{-1}, despite notable differences in geographical location and timing (April, 55° N versus September–November and March–May 52-15° N). Common crane soaring climb rates are comparable to those achieved by griffon vultures (*Gyps fulvus*), an exemplary obligate soarer [44]. Minimum sink rates for the crane and vulture are nearly the same (0.66 versus 0.69 m s^{-1}),

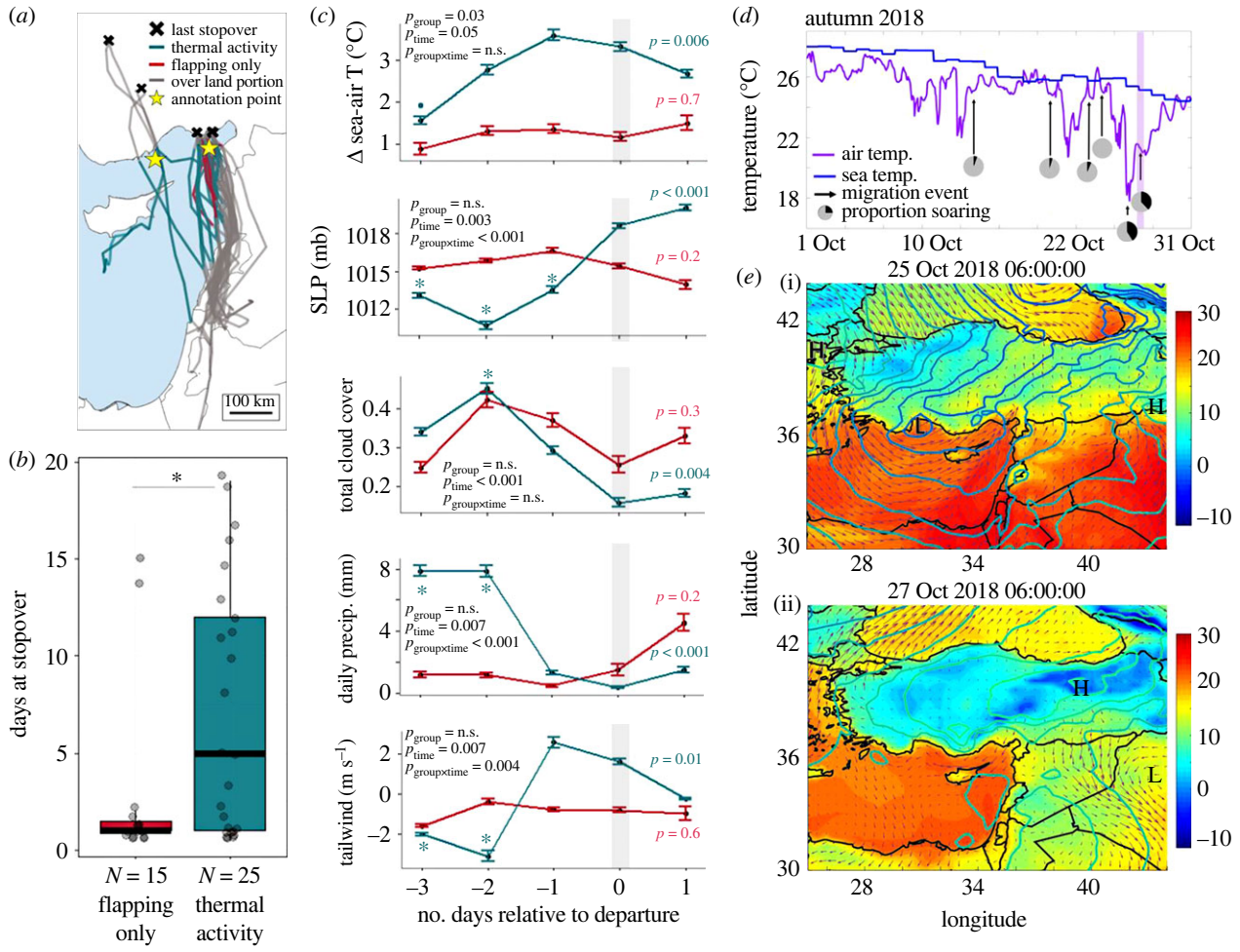

Figure 4. Synoptic analysis of Mediterranean Sea autumn crossing events. (*a*) Map showing all autumn migration tracks that include sections in 1 Hz and cross the Mediterranean Sea. Blue tracks include at least one section with thermal soaring, while red tracks did not include any. In grey are the over land portions of the tracks. Black × denote the last stopover before the sea-crossing migration leg. Yellow stars are the points over the sea used for annotation of meteorological variables for crossings that started from central Turkey (left star) and those that started from Adana, a major stopover site (right star). (*b*) Stopover duration before departure for sea-crossing, for tracks that included at least one section with thermal soaring (blue), and those that did not include any (red). (*c*) Time series of 5 days, with 0 being the day of departure from the stopover sites in Turkey (black × in panel (*a*)). Blues lines are for crossing events that included thermal soaring, while red lines are for crossing events that did not include thermal soaring. Positive Δ sea-air temperature indicates cold air over a warm sea which is necessary for thermals to develop. Total cloud cover ranges between 0 (clear skies) and 1 (complete cloud cover). Tailwind is relative to travel direction. RM-ANOVA results shown of each meteorological factor on bird flight mode (group) and timing (time). One-way ANOVA results are shown above the line in a matching colour, and the analysis was performed to test the timing effect on each flight mode separately. *p*-values for Dunnetts' pairwise comparisons between a certain time and departure time, performed for flight mode found to have a significant effect, are shown (* $p < 0.05$,° $p = 0.07$). (*d*) Time series of sea surface temperature (°C) in blue, and 2 m air temperature (°C) in purple exemplifying conditions during October 2018. Arrows indicate Mediterranean Sea-crossing events; the corresponding pie charts show, in black, the percentage of crossing time that contained thermal soaring. Purple shading indicates the event for which weather conditions are shown in *e*. (*e*) Example of a low-pressure weather system affecting the eastern Mediterranean on 25–27 October 2018. Shaded areas are air temperature (°C) at 2 m height; coloured lines are isobars of sea-level pressure (mb), with colder (bluer) colours indicating lower pressure; and arrows are wind vectors at an altitude of 950 mb (approximately 450 m a.s.l.). 'L' and 'H' indicate low- and high-pressure areas, respectively. (i) 25 October 2018 (−2 timescales relative to departure), 06.00 UTC: a relatively deep low-pressure area approaches the eastern Mediterranean from the west. (ii) 27 October 2018 (departure day), 06.00 UTC, the low-pressure area moved eastward and was replaced by high pressure over Turkey and a shallow insignificant low south-east of Cyprus. SLP, sea level pressure.

hence both could potentially use thermals of similar strength. The same holds also for white storks, with an estimated minimum sink rate of 0.64 m s^{-1}. These comparisons lend further support to our suggestion that thermal strength is not a limiting factor over the sea, but rather the inability of obligate soaring birds to flap substantially between thermals in order to cope with their lower frequency over the sea, as the cranes are able to do. Our findings also support previous observations that cranes merge soaring-gliding and flapping flight to 'prolong' inter-thermal gliding, but occasionally flap also during thermal circling to keep in tight flock formation [10,28]. By keeping formation as they exit the thermal, cranes can conserve energy by formation-flying [45] as soon as they switch from pure gliding to flapping. The higher climb rates and lower flap rates observed during migration over land at southern latitudes probably reflect stronger thermal activity; this allows to preserve energy by relying less on costly flapping flight while crossing these desert areas that have few, if any, opportunities to refuel [10,40].

Mediterranean Sea-crossing events in autumn that included thermal soaring occurred on average 2 days after the passage of mid-latitude cyclones, when positive ΔT values occurred but the precipitation and headwinds associated with the cold front have ceased (figure 4). The low-

pressure area draws in cold air behind it, which increases sea-air ΔT as the sea surface temperature is hardly affected by synoptic variations (figure 4*d*). Winds also tend to have a strong southerly component ahead of the low, which generates headwinds for the south-bound cranes. After the passing of the cold front and during gradual clearing of the low, the northerly (tail) component of the wind sets in, though precipitation may still linger and hinder crane departure. After that, even as ΔT somewhat decreases from its maximum, meteorological conditions are favourable for departure and for thermal soaring over the sea. During the spring, however, the same post-cyclonic cold air events generally correspond to headwinds for the north-bound cranes. This may partly explain why soaring over the Mediterranean was much rarer in spring. The finding that cranes crossing the Mediterranean using thermal soaring tended to wait longer at the last stopover site before crossing could indicate waiting for good soaring conditions, or simply waiting for adverse weather conditions to improve, as there is a connection between the two. It might also suggest that cranes that cross by flapping aim to minimize migration time rather than energy during this part of the migration route, so they are less keen on waiting at the stopover. In addition, high sea-air ΔT is not limited to daytime as thermal updrafts over-land are, and night-time oceanic mesoscale cellular convection is known to form [46]. This could potentially enable birds to soar over sea also during the night. Pennycuick *et al*. [28] noted that common cranes fly across the Mediterranean at night and assumed (whether night- or daytime) they do so by flapping. While we do not have high-resolution data from night-time sea-crossings of cranes, the possibility of soaring during the night cannot be ruled out.

In summary, we provide direct evidence based on rich high-resolution data for routine thermal soaring over the sea in the heaviest facultative soarer among terrestrial migrating birds, which calls to reconsider a prevailing paradigm in bird migration research. The mechanisms underlying this surprising finding encompass the flight mode flexibility of cranes which in turn allows greater flexibility in migration route and timing, as well as the atmospheric processes that enable thermal soaring of such heavy birds over the sea. These atmospheric processes, associated with marine cold air outbreaks, have been given much attention in atmospheric science as they are imperative to understanding low cloud formation and the global energy budget and climate system [29,30,47]. Here, we show that even small-scale marine cold air outbreaks such as those occurring in the eastern Mediterranean and Black Seas, which may not even generate visible convective cells (organized clouds) that are of interest to the atmospheric science community, still have significant global effects for biological processes such as bird migration and are of interest to the biological science community. Our high-resolution tracking of migrating common cranes allowed insights to be gained on the existence and strength of atmospheric thermals over the sea, a micrometeorological-scale phenomenon that cannot be captured by large-scale models and difficult to investigate by human-operated sensors over open sea. Indeed, migratory birds can serve as sentinels of climatological and meteorological phenomena [48,49], sparking new opportunities for multi-disciplinary research across biological and atmospheric sciences.

4. Material and methods

(a) Tagging and data collection

Between January 2016 and September 2018, 44 common cranes (electronic supplementary material, S1) were trapped in their pre-migration flocking areas in western Russia (Ryazan area; 54°56′ N, 41°02 E). The cranes were trapped using alpha-chloralose [cf. 50–52] and processed in accordance with protocols approved by the Department of Environment of the Ryazan district, Russia (permit CK19-7154). Captured birds were colour-ringed, fitted with leg-mounted solar-powered GPS-Global System for Mobile Communications (GSM) transmitters (Orni-Track-L40: Ornitela, Lithuania), morphological measurements were taken, and body feathers were collected for molecular sexing. The maximal total mass of a transmitter plus rings used for attachment was (mean ± s.d.) 0.8 ± 0.09% (range: 0.7–1%; 35–42 g) of the captured cranes' average body mass. Each transmitter included a high-frequency three-dimensional accelerometer and magnetometer sensor.

GPS locations were sampled at a resolution of 2 min to 1 h over the whole annual cycle depending on the measurement scheme and battery recharge. Once a bird was flying inside pre-set geographical areas along the migratory route, GPS data were sampled continuously at 1 s intervals (electronic supplementary material, appendix figure S1). During 1 Hz GPS recording, three-dimensional acceleration and magnetometer data were recorded in synchrony with the GPS position (figure 3*b*). Higher resolution (10 Hz) 4 s bursts of three-dimensional acceleration and magnetometer were recorded once every 1 min; during this ultra-high resolution sensor burst, GPS recording is paused. All data were downloaded remotely through a GSM network connection.

In all our analyses, we used data from individuals migrating mainly along the Russian-Pontic route of the East Eurasian Flyway, leading from breeding grounds in Eastern Europe and the European part of Russia, through the Black Sea and towards wintering grounds in the Near East and north-east Africa [53] (figure 2*a*). A smaller portion of individuals breeding in the European part of Russia also use the Caucasus Flyway, leading across the Caucasus mountains to wintering grounds in Iran, the Near East and north-east Africa [40,53]. Age categories were assigned separately for every migration year, leading to some individuals being included in juvenile category during the first year of data collection and later assigned to the adult category. All movement data analyses were performed using MATLAB R2020a (The Mathworks Inc., Natick, MA, USA).

(b) Movement analysis

High-resolution (1 Hz) data were recorded for various lengths of time depending on battery recharge and point of entry/exit to/from the predefined preset geographical areas. We included in the analysis only continuous 1 Hz sections longer than 10 min. This data filtering resulted in a total of 1352 sections of 71.2 (range: 10–470) min. During the 4 s recording of 10 Hz sensor burst, the 1 Hz GPS recording did not occur. Thus, to create continuous 1 Hz data series, we subsampled the 10 Hz data by selecting the first acceleration and magnetometer value of every second during the burst. Linear interpolation was used to fill the 4 s gaps in GPS data occurring during sensor burst. While dead-reckoning provides a more accurate approach to fill data gaps [54], linear interpolation is not expected to introduce a significant bias in the current study due to the overall low proportion of gaps (6 ± 3% of all data) and the highly similar distribution at different regions.

(c) Identifying thermal soaring-gliding

Soaring-gliding events consist of an altitudinal gain phase performed using circular thermal climbing, followed by a gliding

phase during which altitude loss occurs [55]. Thermal soaring and inter-thermal gliding fundamental movement elements (FMEs) [56] were defined separately in our dataset due to the tendency of the cranes to use a mixture of gliding and flapping flight [10], hence not all thermal soaring phases were followed by clearly definable gliding phases.

To identify soaring phases, we first found all climbing events. Two main types of thermal soaring were observed in our data: (1) classic soaring, or circling flight phases, were identified by a continuous change in heading angle in one direction for at least two full circles during the climb event (97% of all thermal sections) and (2) spring-like soaring pattern, which might be a result of circling with high drift (3% of all thermal sections, 12% of thermal sections over the sea, electronic supplementary material, appendix, figure S3). Those were identified by a continuous change in heading direction using the magnetometer data (figure 3). For each local minimum point in the flight height, we found its following local maximum point. If the time between the max and min points was at least 30 s, and if for each recorded flight heights 10 s apart the latter was higher, we considered it a climb. Climbs less than 15 s apart were merged. A consequent gliding phase was registered if 80% of the 1 s steps were downwards without circling for at least 30 s and if it followed a soaring phase by less than 60 s [55].

The mean (± s.d.) time of thermal soaring was 213 (± 116) s, and the mean (± s.d.) time of gliding was 109 (± 82) s. For each segment of thermal soaring, we calculated vertical speed (climb rate), thermal starting and exit heights above terrain, and flapping proportion (see below). When a matching gliding phase was coupled with the soaring phase (61% of the soaring FMEs), time of gliding, ground speed, air speed, vertical speed (sink speed) and flapping rate (see below) were calculated (figure 3). The minimum sink rate for the common crane was calculated using the FLIGHT (version 1.25) software [42], with crane morphological input values (mean body mass = 5.614 kg, wing area = 0.5853 m^2, wing span = 2.22 m, aspect ratio = 8.42) obtained from data provided in [39].

(d) Flapping rate

The recorded raw tri-axial acceleration (in millivolts) was transformed to actual acceleration (m s^{-2}) using sensor-specific calibration values for each axis obtained prior to deployment of each transmitter. To obtain vertically aligned acceleration, we calculated tri-axial static acceleration and projected the raw acceleration. Our goal was to determine flap rate (number of wingbeats per second) for the entire FME (samples at 1 Hz) and not only for the ultra-high resolution (10 Hz) 4 s acceleration bursts which were sampled intermittently (electronic supplementary material, appendix figure S2). Since commonly used methods [24,57] for determining the flap rate during flight using acceleration data are not suitable at the sampling resolution of 1 Hz because wingbeats occur in a higher temporal resolution, we developed a model to estimate flap rate from 1 Hz data based on a calibration dataset of 10 Hz.

The model was based on a two-layer, fully connected, feed-forward neural network (Python 3.9; TensorFlow 2.8). The input neurons were the result of applying aggregate functions and calculating the Pearson correlation between axes for acceleration and magnitude data. For model calibration, we used 12 580 sections of ultra-high resolution (10 Hz) 4 s acceleration bursts (electronic supplementary material, appendix figure S2A), divided into 80% for model training and 20% for model validation. For each section, flap rate was calculated by identifying wingbeats represented as peaks at the heave axis [cf. 25] and dividing the number of peaks by 4 s (section total length). Models were estimated for multiple configurations and the best model was selected according to the goodness-of-fit of the flap rate projected from 1 Hz data and the one calculated from 10 Hz data. The best-performing model ($R^2 = 0.91$) was based on five continuous samples (4 s) of 1 Hz acceleration (magnitude data were dropped in model selection) with the flap rate estimated for the middle sample point. This model was used to calculate flap rate from 1 Hz data for all our tracks (figure 3; electronic supplementary material, figure S2B). The mean (± s.d.) calculated flap rate was 2.15 (± 0.79) flaps s^{-1} during powered flapping flight and 0.89 (± 0.83) flaps s^{-1} during thermal soaring.

Flapping rate was converted into flapping ratio (number of wingbeats out of the maximal number of wingbeats expected during flapping flight) to better represent flapping behaviour during each FME. Flapping ratio was calculated by dividing the cumulative number of flaps in each FME by the maximal possible number of flaps based on the mean calculated flapping rate during powered flight. This method of flapping ratio calculation probably leads to overestimation of flapping, as a particular second is considered flapping regardless of how many wing flaps were performed in that second [24,25]. However, because the actual number of flaps was unknown and estimated based on a running average over 4 s, our calculation is representative of the flapping ratio during the different movement phases.

(e) Annotating environmental variables

Flight height above ground level was calculated by subtracting from the altitude above sea level [58] the ground elevation (ASTER DEM, 1 arc-second spatial resolution) obtained from Env-DATA track annotation service [20]. To relate the flight behaviour to the time of day, we classified diurnal locations as those collected between sunrise and sunset and regarded the remaining locations as nocturnal. To identify flight above the Black Sea and Mediterranean Sea, we used the Marine Regions shapefile [59] and annotated the corresponding position to the location inside or outside the polygon.Sea-crossing was identified if at least one point was located inside the sea polygon. All data tracks were classified to three geographical areas: (a) over Black or Mediterranean Seas, (b) over land north of latitude 32°N and (c) over land south of latitude 32°N. Latitude 32°N was chosen to differentiate tracks above desert or elsewhere because the geographical areas in which the 1 Hz data was sampled do not include deserts north of this latitude (electronic supplementary material, appendix figure S1).

Atmospheric variables were obtained from the ERA5 hourly data on pressure levels [60] and single levels [61] from 1979 to present, provided by European Centre for Medium-Range Weather Forecasts (ECMWF). We annotated all crane GPS locations with the following single-level variables: mean sea level pressure, air temperature at 2 m above the surface, sea surface temperature, total cloud cover and boundary layer height (BLH). Additionally, annotation was done on the 950 millibar pressure level with geopotential height and U- and V- wind components. Since the ERA5 temporal resolution is 1 h, the GPS location timestamp was rounded to the nearest hour for the ERA5 annotation. Precipitation data were obtained from the GPCC First Guess Daily Product at 1.0° [62].

(f) Statistical analysis

To assess thermal soaring under different conditions, we segmented the data into 10 min sections and only sections lasting 10 full minutes were analysed. The sections were classified as above sea or above land and only sections for which all points were classified to the same habitat were analysed. For this analysis, only thermal soaring was considered and for each section, the number of thermal soaring FMEs and total time in thermal soaring were recorded.

To identify factors influencing thermal probability at sea, we modelled the relationship between thermal presence and meteorological predictor variables using binomial generalized linear-mixed model (GLMM) with the glmer function in the *lme4* package [63]. Before fitting the GLMMs, all continuous predictors were transformed to *z*-scores to standardize them [64]. To rule out collinearity, we calculated Pearson's correlation coefficients (r) between each pair of explanatory variables and selected variables with $|r|$ less than 0.7 [65] We compared the full model with a null model (including only random and control variables) using likelihood-ratio tests (ANOVA function set to 'Chisq'). The response variable was presence/absence of thermal circling, and the predictor meteorological variables included wind speed, mean temperature difference between sea and air (ΔT) and sea level pressure. Mean BLH was correlated with ΔT ($r = 0.72$, $p < 0.001$) and excluded from the model. An additional predictor variable was individual age (categorized as 'adults' versus 'subadults'—birds under the age of three). First year juveniles were not analysed separately because our dataset included only one juvenile. Animal ID was included as a random factor in all models to account for repeated measures.

To compare the proportion of 10 min sections with and without thermal presence at different geographical regions and between autumn and spring, we applied binomial GLMM with logit link function in the '*lme4*' package [63]. Season (categorized as 'autumn' and 'spring') and geographical regions (categorized as 'North', 'Desert', 'Sea') were included as fixed factors while crane ID was a random factor. Likelihood ratio tests (LRTs) were used to test for significance of explanatory variables. *Post hoc* comparisons of the estimated marginal effects were conducted using the R package *emmeans*, with Holm step-down procedure for multiple comparisons. To compare time soaring, we analysed only trips (continuous flight event) with at least one thermal soaring event. We analysed the difference in the proportion of time in soaring flight in the different geographical regions, using Aligned Rank Transformed ANOVA (ART-ANOVA) for our non-parametric, factorial analyses, due to the non-convergence of a binomial GLMM, likely attributed to data sparsity after aggregation by trip. This approach was implemented using the *ARTool* package [66] with geographical region as a fixed factor and crane ID as a random factor. We conducted within-group comparisons using the *ARTool* pairwise contrast function and between-group comparisons using Mann–Whitney U-tests with Tukey corrected *p*-values. Similarly, ART-ANOVA was used to compare flap ratio during climbing and gliding, climb rate and exit height (above ground level) from thermals, between the different geographical regions. For this analysis, only coupled soaring-gliding FMEs were used.

We used repeated measures analysis of variance (RM-ANOVA) to compare conditions in the Mediterranean Sea across different timescales relative to the autumn departure of cranes for sea-crossing. We considered time (up to 3 days prior to departure and 1 day after) as a within-subject factor and flight mode (soaring or flapping) as a between-subject factor (after [67]). Crossing flight mode was set as thermal soaring if at least one 10 min section with thermal soaring was present during crossing; otherwise, it was set as flapping only. Each meteorological factor (ΔT, sea level pressure, total cloud cover, precipitation and tailwind) was analysed separately. For annotation of meteorological conditions two common locations at sea were selected for birds departing from central Turkey (36°08′ N, 34°06 E) and Adana (35°17′ N, 35°36 E), respectively (figure 4*a*) and at the time the birds entered the Mediterranean Sea. Tailwind was calculated in relation to bird flight direction between the point of departure and the point of analysis in sea. We performed a one-way ANOVA for each meteorological factor within each flight mode group separately to determine if there were significant differences across timescales. Subsequently, for cases where significant time effects were observed, we applied Dunnett's test [68] to compare the conditions at the departure day with the ones measured at other days (−3, −2, −1 and +1).

Ethics. The cranes were trapped and processed in accordance with protocols approved by the Department of Environment of the Ryazan district, Russia (permit CK19-7154) and the Israel Nature and Parks Authority (permit 2015/41169). The animal experimental protocol was approved by the ethics review committee of The Hebrew University of Jerusalem (NIH approval number: OPRR-A01-5011).

Data accessibility. All data and scripts associated with this manuscript are available on Dryad Digital Repository: https://doi.org/10.5061/dryad.t76hdr871 [69].

Additional information is provided in electronic supplementary material [70].

Declaration of AI use. We have not used AI-assisted technologies in creating this article.

Authors' contributions. S.P.: conceptualization, formal analysis, investigation, methodology, project administration, visualization, writing—original draft, writing—review and editing; D.S.: formal analysis, writing—original draft, writing—review and editing; N.H.: software, writing—review and editing; R.C.B.: funding acquisition, writing—review and editing; P.K.: funding acquisition, writing—review and editing; Y.M.: methodology, writing—review and editing; W.M.G.: funding acquisition, writing—review and editing; R.N.: conceptualization, funding acquisition, project administration, supervision, writing—review and editing.

All authors gave final approval for publication and agreed to be held accountable for the work performed therein.

Conflict of interest declaration. We declare we have no competing interests.

Funding. This research was funded by BSF grant no. 904/2015 to R.N. and W.M.G., by GIF grant no. 999-66.8/2008, ISF grant no. 2525/16 and JNF/KKL grant no. 14-093-01-6 to R.N., and by NSF grant no. 1617982 to W.M.G., R.C.K.B. and P.L.K. We also acknowledge financial support from the Adelina and Massimo Della Pergola Chair of Life Sciences and the Minerva Center for Movement Ecology to R.N.

Acknowledgements. The authors wish to thank to K. Postelnykh, K. Kondrakova, N.Yesraeli, S. Agmon, Y. Charka, G. Shani, N. Valtzer and F. Argyle for help in fieldwork and trapping. We also thank the members of Nathan's Movement Ecology laboratory and especially Y. Bartan and S. Turjeman for their help at various stages of the research.

References

1. Nathan R, Getz WM, Revilla E, Holyoak M, Kadmon R, Saltz D, Smouse PE. 2008 A movement ecology paradigm for unifying organismal movement research. *Proc. Natl Acad. Sci. USA* **105**, 19052. (doi:10.1073/pnas.0800375105)
2. Alerstam T. 2011 Optimal bird migration revisited. *J. Ornithol.* **152**, 5–23. (doi:10.1007/s10336-011-0694-1)
3. Moreau RE. 1972 *The Palaearctic-African bird migration systems*. London, UK: Academic Press.
4. Newton I. 2008 *The migration ecology of birds*. Oxford, UK: Academic Press.
5. Alerstam T, Hedenström A, Åkesson S. 2003 Long-distance migration: evolution and determinants. *Oikos* **103**, 247–260. (doi:10.1034/j.1600-0706.2003.12559.x)
6. Alerstam T. 2001 Detours in bird migration. *J. Theor. Biol.* **209**, 319–331. (doi:10.1006/jtbi.2001.2266)
7. Pennycuick CJ. 1972 Soaring behaviour and performance of some east African birds, observed from a motor-glider. *Ibis* **114**, 178–218. (doi:10.1111/j.1474-919X.1972.tb02603.x)
8. Hedenström A. 1993 Migration by soaring or flapping flight in birds: the relative importance of

energy cost and speed. *Phil. Trans. R. Soc. B* **342**, 353–361. (doi:10.1098/rstb.1993.0164)

9. Pennycuick CJ. 1969 The mechanics of bird migration. *Ibis* **111**, 525–556. (doi:10.1111/j.1474-919X.1969.tb02566.x)
10. Alerstam T. 1993 *Bird migration*. Cambridge, UK: Cambridge University Press.
11. Bildstein KL. 2006 *Migrating raptors of the world: their ecology and conservation*. Ithaca, NY: Cornell University Press.
12. Shamoun-Baranes J, Bouten W, van Loon EE, Meijer C, Camphuysen CJ. 2016 Flap or soar? How a flight generalist responds to its aerial environment. *Phil. Trans. R. Soc. B* **371**, 20150395. (doi:10.1098/rstb.2015.0395)
13. Vansteelant WMG, Bouten W, Klaassen RHG, Koks BJ, Schlaich AE, van Diermen J, van Loon EE, Shamoun-Baranes J. 2015 Regional and seasonal flight speeds of soaring migrants and the role of weather conditions at hourly and daily scales. *J. Avian Biol.* **46**, 25–39. (doi:10.1111/jav.00457)
14. Shamoun-Baranes J, Liechti F, Vansteelant WMG. 2017 Atmospheric conditions create freeways, detours and tailbacks for migrating birds. *J. Comp. Physiol. A* **203**, 509–529. (doi:10.1007/s00359-017-1181-9)
15. Shamoun-Baranes J, van Loon E, van Gastere H, van Belle J, Bouten W, Buurma L. 2006 A comparative analysis of the influence of weather on the flight altitudes of birds. *Bull. Am. Meteorol. Soc.* **87**, 47–62. (doi:10.1175/BAMS-87-1-47)
16. Agostini N, Panuccio M, Pasquaretta C. 2015 Morphology, flight performance, and water crossing tendencies of Afro-Palearctic raptors during migration. *Cur. Zool.* **61**, 951–958. (doi:10.1093/czoolo/61.6.951)
17. Mellone U. 2020 Sea crossing as a major determinant for the evolution of migratory strategies in soaring birds. *J. Anim. Ecol.* **89**, 1298–1301. (doi:10.1111/1365-2656.13241)
18. Rayner JM. 1988 Form and function in avian flight. In *Current ornithology*, vol. 5 (ed R.F. Johnston), pp. 1–66. Boston, MA; Berlin, Germany: Springer.
19. Norberg UML. 2002 Structure, form, and function of flight in engineering and the living world. *J. Morph* **252**, 52–81. (doi:10.1002/jmor.10013)
20. Dodge S *et al.* 2014 Environmental drivers of variability in the movement ecology of turkey vultures (*Cathartes aura*) in North and South America. *Phil. Trans. R. Soc. B* **369**, 20130195. (doi:10.1098/rstb.2013.0195)
21. Flack A *et al.* 2016 Costs of migratory decisions: a comparison across eight white stork populations. *Sci. Adv.* **2**, e1500931. (doi:10.1126/sciadv.1500931)
22. Phipps WL *et al.* 2019 Spatial and temporal variability in migration of a soaring raptor across three continents. *Front. Ecol. Evol.* **7**, 323. (doi:10.3389/fevo.2019.00323)
23. Becciu P *et al.* 2020 Causes and consequences of facultative sea crossing in a soaring migrant. *Funct. Ecol.* **34**, 840–852. (doi:10.1111/1365-2435.13539)
24. Rotics S *et al.* 2016 The challenges of the first migration: movement and behaviour of juvenile vs. adult white storks with insights regarding juvenile mortality. *J. Anim. Ecol.* **85**, 938–947. (doi:10.1111/1365-2656.12525)
25. Rotics S *et al.* 2017 Corrigendum. *J. Anim. Ecol.* **86**, 1281. (doi:10.1111/1365-2656.12704)
26. Spaar R. 1997 Flight strategies of migrating raptors; a comparative study of interspecific variation in flight characteristics. *Ibis* **139**, 523–535. (doi:10.1111/j.1474-919X.1997.tb04669.x)
27. Mellone U, Lucia G, Mallìa E, Urios V. 2016 Individual variation in orientation promotes a 3000-km latitudinal change in wintering grounds in a long-distance migratory raptor. *Ibis* **158**, 887–893. (doi:10.1111/ibi.12401)
28. Pennycuick CJ, Alerstam T, Larsson B. 1979 Soaring migration of the common crane *Grus grus* observed by radar and from an aircraft. *Ornis Scandinavica (Scandinavian Journal of Ornithology)* **10**, 241–251. (doi:10.2307/3676068)
29. Agee EM. 1987 Mesoscale cellular convection over the oceans. *Dyn. Atmos. Oceans* **10**, 317–341. (doi:10.1016/0377-0265(87)90023-6)
30. Atkinson BW, Zhang WJ. 1996 Mesoscale shallow convection in the atmosphere. *Rev. Geophys.* **34**, 403–431. (doi:10.1029/96RG02623)
31. Stevens B. 2004 Atmospheric moist convection. *Annu. Rev. Earth Planet. Sci.* **33**, 605–643. (doi:10.1146/annurev.earth.33.092203.122658)
32. Weimerskirch H, Bishop C, Jeanniard-du-Dot T, Prudor A, Sachs G. 2016 Frigate birds track atmospheric conditions over months-long transoceanic flights. *Science* **353**, 74. (doi:10.1126/science.aaf4374)
33. Woodcock AH. 1940 Convection and soaring over the open sea. *J. Mar. Res.* **3**, 248–253.
34. Woodcock AH. 1975 Thermals over the sea and gull flight behavior. *Boundary Layer Meteorol.* **9**, 63–68. (doi:10.1007/BF00232254)
35. Yamaguchi NM, Arisawa Y, Shimada Y, Higuchi H. 2012 Real-time weather analysis reveals the adaptability of direct sea-crossing by raptors. *J. Ethol.* **30**, 1–10. (doi:10.1007/s10164-011-0301-1)
36. Nourani E, Vansteelant WMG, Byholm P, Safi K. 2020 Dynamics of the energy seascape can explain intra-specific variations in sea-crossing behaviour of soaring birds. *Biol. Lett.* **16**, 20190797. (doi:10.1098/rsbl.2019.0797)
37. Nourani E *et al.* 2021 The interplay of wind and uplift facilitates over-water flight in facultative soaring birds. *Proc. R. Soc. B* **288**, 20211603. (doi:10.1098/rspb.2021.1603)
38. Duriez O, Peron G, Gremillet D, Sforzi A, Monti F. 2018 Migrating ospreys use thermal uplift over the open sea. *Biol. Lett.* **14**, 20180687. (doi:10.1098/rsbl.2018.0687)
39. Alerstam T, Rosén M, Bäckman J, Ericson PGP, Hellgren O. 2007 Flight speeds among bird species: allometric and phylogenetic effects. *PLoS Biol.* **5**, e197. (doi:10.1371/journal.pbio.0050197)
40. Ojaste I, Leito A, Suorsa P, Hedenström A, Sepp K, Leivits M, Sellis U, Väli Ü. 2020 From northern Europe to Ethiopia: long-distance migration of common cranes (*Grus grus*). *Ornis Fennica* **97**, 12–25. (doi:10.51812/of.133962)
41. Alerstam T. 1975 Crane *Grus grus* migration over sea and land. *Ibis* **117**, 489–495. (doi:10.1111/j.1474-919X.1975.tb04241.x)
42. Pennycuick CJ. 2008 *Modelling the flying bird*. Burlington, MA: Academic Press.
43. Pennycuick CJ. 1983 Thermal soaring compared in three dissimilar tropical bird species, *Fregata Magnificens*, *Pelecanus Occidentals* and *Coragyps Atratus*. *J. Exp. Biol.* **102**, 307–325. (doi:10.1242/jeb.102.1.307)
44. Harel R, Nathan R. 2018 The characteristic time-scale of perceived information for decision-making: departure from thermal columns in soaring birds. *Funct. Ecol.* **32**, 2065–2072. (doi:10.1111/1365-2435.13136)
45. Portugal SJ, Hubel TY, Fritz J, Heese S, Trobe D, Voelkl B, Hailes S, Wilson AM, Usherwood JR. 2014 Upwash exploitation and downwash avoidance by flap phasing in ibis formation flight. *Nature* **505**, 399–402. (doi:10.1038/nature12939)
46. Miller MA, Albrecht BA. 1995 Surface-based observations of mesoscale cumulus–stratocumulus interaction during ASTEX. *J. Atmos. Sci.* **52**, 2809–2826. (doi:10.1175/1520-0469(1995)052<2809:SBOOMC>2.0.CO;2)
47. Fletcher J, Mason S, Jakob C. 2016 The climatology, meteorology, and boundary layer structure of marine cold air outbreaks in both hemispheres. *J. Clim.* **29**, 1999–2014. (doi:10.1175/JCLI-D-15-0268.1)
48. Treep J, Bohrer G, Shamoun-Baranes J, Duriez O, Prata de Moraes Frasson R, Bouten W. 2016 Using high-resolution GPS tracking data of bird flight for meteorological observations. *Bull. Am. Meteorol. Soc.* **97**, 951–961. (doi:10.1175/BAMS-D-14-00234.1)
49. Shepard ELC. 2022 Energy economy in flight. *Curr. Biol.* **32**, R672–R675. (doi:10.1016/j.cub.2022.02.004)
50. Hartup BK, Schneider L, Engels JM, Hayes MA, Barzen JA. 2014 Capture of sandhill cranes using alpha-chloralose: a 10-year follow-up. *J. Wildl Dis.* **50**, 143–145. (doi:10.7589/2013-06-140)
51. Markin YM. 2013 *Eurasian crane in the European part of Russia*. In: Proceedings of the Oka State Nature Biosphere Reserve 29, p. 118 (ed. V. Ivanchev). Ryazan, Russia: NP "Golos Gubernii".
52. Hayes MA, Hartup BK, Pittman JM, Barzen JA. 2003 Capture of sandhill cranes using alpha-chloralose. *J. Wildl Dis.* **39**, 859–868. (doi:10.7589/0090-3558-39.4.859)
53. Mirande C, Harris J. 2019 *Crane conservation strategy*. Baraboo, WI: International Crane Foundation.
54. Bidder OR *et al.* 2015 Step by step: reconstruction of terrestrial animal movement paths by dead-reckoning. *Mov. Ecol.* **3**, 23. (doi:10.1186/s40462-015-0055-4)

55. Horvitz N, Sapir N, Liechti F, Avissar R, Mahrer I, Nathan R. 2014 The gliding speed of migrating birds: slow and safe or fast and risky? *Ecol. Lett.* **17**, 670–679. (doi:10.1111/ele.12268)
56. Getz WM, Saltz D. 2008 A framework for generating and analyzing movement paths on ecological landscapes. *Proc. Natl Acad. Sci. USA* **105**, 19066. (doi:10.1073/pnas.0801732105)
57. Efrat R, Harel R, Alexandrou O, Catsadorakis G, Nathan R. 2019 Seasonal differences in energy expenditure, flight characteristics and spatial utilization of Dalmatian Pelicans *Pelecanus crispus* in Greece. *Ibis* **161**, 415–427. (doi:10.1111/ibi.12628)
58. Poessel SA, Duerr AE, Hall JC, Braham MA, Katzner TE. 2018 Improving estimation of flight altitude in wildlife telemetry studies. *J. Appl. Ecol.* **55**, 2064–2070. (doi:10.1111/1365-2664.13135)
59. Flanders Marine Institute. 2018 IHO Sea Areas, version 3. Available online at http://www.marineregions.org/.
60. Hersbach H *et al.* 2018 ERA5 hourly data on pressure levels from 1979 to present. Copernicus Climate Change Service (C3S) Climate Data Store (CDS).
61. Hersbach H *et al.* 2018 ERA5 hourly data on single levels from 1979 to present. Copernicus Climate Change Service (C3S) Climate Data Store (CDS).
62. Schamm K, Ziese M, Becker A, Finger P, Meyer-Christoffer A, Rudolf B, Schneider U. 2013 Gpcc First Guess Daily Product at 1.0°: near real-time first guess daily land-surface precipitation from rain-gauges based on synop data. (doi:10.5676/DWD_GPCC/FG_D_100)
63. Bates D, Mächler M, Bolker B, Walker S. 2015 Fitting linear mixed-effects models using lme4. *J. Stat. Softw.* **67**, 1–48. (doi:10.18637/jss.v067.i01)
64. Schielzeth H. 2010 Simple means to improve the interpretability of regression coefficients. *Methods Ecol. Evol.* **1**, 103–113. (doi:10.1111/j.2041-210X.2010.00012.x)
65. Dormann CF *et al.* 2013 Collinearity: a review of methods to deal with it and a simulation study evaluating their performance. *Ecography* **36**, 27–46. (doi:10.1111/j.1600-0587.2012.07348.x)
66. Wobbrock JO, Findlater L, Gergle D, Higgins JJ. 2011 *The aligned rank transform for nonparametric factorial analyses using only anova procedures*. In *Proc. of the 2011 Annual Conf. on Human factors in Computing Systems - CHI '11*. New York, NY: ACM Press.
67. Sapir N, Wikelski M, Avissar R, Nathan R. 2011 Timing and flight mode of departure in migrating European bee-eaters in relation to multi-scale meteorological processes. *Behav. Ecol. Sociobiol.* **65**, 1353–1365. (doi:10.1007/s00265-011-1146-x)
68. Dunnett CW. 1955 A multiple comparison procedure for comparing several treatments with a control. *J. Am. Stat. Assoc.* **50**, 1096–1121. (doi:10.1080/01621459.1955.10501294)
69. Pekarsky S, Shohami D, Horvitz N, Bowie Rck, Kamath P L, Markin Y, Getz W M, Nathan R. 2024 Cranes soar on thermal updrafts behind cold fronts as they migrate across the sea. Dryad Digital Repository. (doi:10.5061/dryad.t76hdr871)
70. Pekarsky S, Shohami D, Horvitz N, Bowie RCK, Kamath PL, Markin Y, Getz WM, Nathan R. 2024 Cranes soar on thermal updrafts behind cold fronts as they migrate across the sea. Figshare. (doi:10.6084/m9.figshare.c.6991992)